Polyamine Transport Is Required for Stress Responses and Capsule Production in Streptococcus Pneumoniae

Mary F. Nakamya
Mississippi State University
Moses B. Ayoola
Mississippi State University
Leslie A. Shack
Mississippi State University
Edwin Swiatlo
Southeast Louisiana Veterans Health Care System
Bindu Nanduri (bnanduri@cvm.msstate.edu)
Department of Comparative Biomedical Sciences, College of Veterinary Medicine, P.O. Box 6100, Mississippi State, MS 39762, USA; mfn35@msstate.edu (M.F.N.); mba185@msstate.edu (M.B. A.), shack@cvm.msstate.edu (L.A.S.)

Research Article

Keywords: Streptococcus pneumoniae, polyamine transporter, oxidative stress, nitrosative stress, transcriptome, metabolome

Posted Date: February 8th, 2021

DOI: https://doi.org/10.21203/rs.3.rs-192362/v1

Abstract

Infections due to *Streptococcus pneumoniae*, a commensal in the nasopharynx, still claim a significant number of lives worldwide. Genetic plasticity, antibiotic resistance, limited serotype coverage of the available polysaccharide-based conjugate vaccines confounds therapeutic interventions. Pathogenic systems that allow successful adaption and persistence in the host could be potential innovative targets for mediations. Polyamines are ubiquitous polycationic molecules and regulate many cellular processes. We previously reported that deletion of *potABCD*, an operon that encodes a putrescine/spermidine transporter (Δ*potABCD*), resulted in an un-encapsulated attenuated phenotype. Here we characterize the transcriptome, metabolome, and stress responses of *S. pneumoniae* that is dependent on the polyamine transporter. Expression of genes involved in oxidative stress responses and the central metabolism was reduced while that of genes involved in the Leloir, tagatose, and pentose phosphate pathways was increased in Δ*potABCD*. Downregulation of genes of the central metabolism will reduce production of precursors of capsule polysaccharides. Metabolomics results show reduced glutathione and pyruvate levels in the mutant. We also show that the *potABCD* operon protects pneumococci against hydrogen peroxide and nitrosative stress. These results show the importance of the *potABCD* operon and polyamine transport in pneumococcal physiology and fitness that represents a novel target for therapeutic interventions.

Introduction

Despite years of intensive research, infections due to *Streptococcus pneumoniae* (pneumococcus) still claim countless lives across the entire globe [1]. Pneumococci account for up to 15% of pneumonia cases in the USA and 27% worldwide [2]. Following colonization of the nasopharynx, pneumococci can translocate to sterile sites and cause infections such as community-acquired pneumonia, meningitis, septicemia and otitis media [3]. Well-coordinated metabolic networks for efficient exploitation of the host micro-nutrients and immune response evasion strategies are crucial for pneumococcal pathogenesis. Serotype diversity, limited serotype coverage of the available vaccines, serotype replacement, and increase in multidrug-resistant strains confound intervention strategies to limit the spread of pneumococci [4–6]. A better understanding of pneumococcal physiology and survival mechanisms in the host can identify novel therapeutic targets.

Polyamines are polycationic molecules that interact with RNA, DNA, and phospholipids and modulate cellular processes such as cell division, transcription, and translation [7, 8]. Putrescine, spermidine and cadaverine are the principal bacterial polyamines and their intracellular concentrations are tightly regulated by transport, biosynthesis, and degradation [8]. In pathogenic bacteria, polyamines are known to regulate virulence, biofilm formation, stress responses, *in vivo* fitness, and host-pathogen interactions [9]. Therefore, failure to sustain intracellular polyamine levels could alter regulatory homeostasis which could interfere with *in vivo* survival and pathogenesis. Our previous work has shown that the polyamine transport operon *potABCD* is essential for virulence in murine models of pneumococcal infections [10]. We have shown that in a murine model of pneumonia, Δ*potABCD* is more invasive than the wild type

strain (WT) but is more susceptible to opsonophagocytosis. Uptake of Δ*potABCD* by neutrophils does not require antibody opsonization [11]. PotD, either alone or in combination with other proteins, has been shown to elicit protection against pneumococcal colonization, pneumonia, and sepsis in mice [12–14]. We have recently shown that deletion of the *potABCD* operon resulted in reduced intracellular concentrations of putrescine and spermidine and an un-encapsulated phenotype [10, 15]. Since pneumococcal capsular polysaccharide (CPS) is a determinant of virulence, reduced CPS could explain reported *in vivo* attenuation of Δ*potABCD*. Initial characterization of the Δ*potABCD* proteome identified altered expression of over 100 proteins including virulence factors such as pneumolysin [10]. However, the limited proteome coverage did not allow for the identification of specific mechanisms of metabolic regulation that could explain the observed phenotype. To determine polyamine dependent metabolic regulation that is at the intersection of pneumococcal virulence, we compared the *Δ potABCD* and WT transcriptome and metabolome using RNA-Seq and metabolomics. Given the role of polyamines in the defense against reactive radicals, and the diversity of stress conditions encountered by pneumococci, reduced intracellular polyamine levels are expected to adversely affect stress responses that are critical for *in vivo* fitness. We therefore, examined the role of polyamine transport on the susceptibility of pneumococci to oxidative and nitrosative stress. We determined the impact of impaired polyamine transport on the intracellular pH (pH_i), GSH/GSSG ratio, and production of Nicotinamide adenine dinucleotide phosphate (NADPH), and hydrogen peroxide (H_2O_2). Our results show that polyamine transport is required for the regulation of stress responses and central metabolism that adversely affect capsular polysaccharide synthesis in pneumococci and present an attractive target for developing novel therapeutics.

Results

Polyamine transport modulates pneumococcal gene expression.

Comparison of the transcriptome profiles of TIGR4 and Δ*potABCD* identified regulatory mechanisms responsive to polyamine transport. We identified a total of 1333 genes whose expression varied significantly in Δ*potABCD.* Expression of 651 and 682 genes was downregulated and upregulated in Δ*potABCD*, respectively (Tables 1–3 and Supp Table 2). Gene Ontology analysis of the differentially expressed genes (DEGs) identified significant enrichment of five categories which included: phosphotransferase systems (PTS), galactose metabolism, ABC transporters, amino and nucleotide sugars as well as fructose and mannose metabolism. Major biological functions and pathways represented by the DEGs with a fold change of ≥ 2 and metabolites are discussed in the following sections and shown in Tables 1–3 and Table 5, respectively.

Polyamine transporter and pneumococcal stress responses.

Polyamines protect cells against reactive oxygen species (ROS) via regulation of stress response genes or by directly scavenging reactive free radicals [8, 16]. Therefore, deficiency of polyamines could impact the redox status and render Δ*potABCD* susceptible to oxidative stress. Downregulation of genes that encode

treR, a scavenger of H_2O_2, molecular chaperones and their regulator, *hrcA* (Table 3), indicate impaired redox and repair systems which could compromise *in vivo* fitness of Δ*potABCD* [17, 18]. Reduced expression of genes that encode several tRNAs (Supp. Table 2) could represent cellular adaptation during stress to meet the demand for redox homeostasis [19]. Increased expression of some genes that encode regulators implicated in pneumococcal stress responses, the arginine deiminase system (ADS) and glutamine transporters could be in response to oxidative stress in the mutant [20, 21] (Table 1). Elevated glutamine influx and ADS could be in response to meet the increased demand for energy (ATP) and to restore the buffering capacity (ammonia). Increased expression of ABC transporters for the import of iron, manganese, and phosphate (Tables 1) could result in cationic imbalance and negatively impact cellular functions and redox homeostasis [22]. These results show that deficiency of the polyamine transporter impairs pneumococcal stress systems, renders the mutant susceptible to oxidative stress and triggers polyamine independent redox systems to combat the stress.

Table 1
The *potABCD* operon is essential for pneumococcal stress responses.

Locus tag	Gene	Fold change Δ*potABCD*/TIGR4	Description
SP_1884	SP_1884	-3.6	PTS trehalose transporter subunit IIBC
SP_1883	SP_1883	-3.2	Trehalose6-phosphate hydrolase
SP_1907	*groES*	-3.9	Co-chaperone
SP_0519	*dnaJ*	-3.8	Molecular chaperone
SP_0517	*dnaK*	-4.2	Molecular chaperone
SP_1906	*groEL*	-3.3	Molecular chaperone
SP_1870	SP_1870	2.7	Iron-compound ABC transporter
SP_1871	SP_1871	2.9	Iron ABC transporter ATP-binding protein
SP_1241	SP_1241	3.1	Glutamine transport system substrate-binding
SP_1242	SP_1242	3.2	Glutamine transport system ATP-binding protein
SP_2087	*pstB*	41.8	Phosphate ABC transporter ATP-binding protein
SP_2085	*pstC*	37.2	Phosphate ABC transporter permease subunit
SP_2084	*pstS*	27.2	Phosphate ABC transporter substrate-binding
SP_2086	*pstA*	40.6	Phosphate ABC transporter permease protein
SP_1650	*psaA*	3.2	Manganese ABC transporter substrate-binding
SP_1648	*psaB*	3.4	Metal ABC transporter ATP-binding protein
SP_1649	*psaC*	3.5	Metal ABC transporter permease
SP_0502	*glnA*	4.2	Glutamine synthetase
SP_2148	*arcA*	4.6	Arginine deiminase
SP_2151	*arcC*	3.7	Carbamate kinase
SP_0798	*ciaR*	3.0	DNA-binding response regulator
SP_0799	*ciaH*	3.0	Two-component sensor histidine kinase
SP_0501	*merR*	4.0	MerR family transcriptional regulator;

Locus tag	Gene	Fold change Δ*potABCD*/TIGR4	Description
SP_0515	*hrcA*	-4.3	Transcriptional regulator
SP_2088	*phoU*	47.2	Phosphate uptake regulator

Galactose utilization and the pentose phosphate pathway (PPP).

The signature of oxidative stress was further revealed by metabolic shift towards the PPP in the mutant which is usually in response to oxidative stress to produce NADH/NADPH which are cofactors in antioxidant systems [23].

Table 2
The *potABCD* operon promotes galactose utilization and the pentose phosphate pathway.

Locus tag	Gene	Fold change Δ*potABCD*/TIGR4	Description
SP_2127	*tktN*	222.7	Transketolase
SP_2128	*tktC*	225.5	Transketolase
SP_2130	*SP_2130*	211.5	Ascorbate PTS system EIIB
SP_2129	*SP_2129*	214.7	PTS ascorbate transporter subunit IIC
SP_1192	*lacB*	2.8	Galactose6-phosphate isomerase subunit
SP_1193	*lacA*	2.8	Galactose6-phosphate isomerase subunit
SP_1190	*lacD*	2.8	Tagatose1,6-diphosphate aldolase
SP_1191	*lacC*	2.8	Tagatose6-phosphate kinase
SP_1186	*lacF-2*	2.0	Lactose PTS system EIIA component
SP_2165	*fucU*	4.5	Fucose isomerase
SP_2166	*fucA*	3.8	L-fuculose phosphate aldolase
SP_1853	*galK*	6.1	Galactokinase
SP_0066	*galM*	2.7	Galactose mutarotase
SP_0064	SP_0064	3.4	PTS mannose PTS system EIIA
SP_0645	SP_0645	8.8	PTS galactose PTS system EIIA
SP_0646	SP_0646	9.0	PTS galactose PTS system EIIB
SP_2164	SP_2164	3.7	PTS mannose transporter subunit IIA
SP_2161	SP_2161	3.3	PTS mannose transporter subunit IID
SP_2162	SP_2162	3.7	PTS mannose PTS system EIIC

Expression of genes that encode enzymes of the Leloir pathway involved in galactose catabolism and generation of UDP-galactose (UDP-Gal) was upregulated in the mutant (Table 2). Expression of lacF-2 and the lacDCBA operon involved in the import and interconversion of galactose via the tagatose pathway to fructose6-phosphate and glyceraldehyde3-phosphate (G3P) was upregulated (Table 2). Upregulated Leloir and tagatose pathways could be in response to high demand for PPP precursors in the mutant. Increased PPP and G3P may contribute to upregulation of tktC and tktN which encode a transketolase that catalyzes the interconversion of sugar-phosphates in the pathway (Table 2). There was an increase in the expression of genes that encode enzymes that degrade fucose (Table 2). Fucose degradation by triosephosphate isomerase yields G3P, an intermediate of glycolysis and PPP [24]. Increased expression of a putative PTS system involved in the import and interconversion of L-ascorbate to xylulose5-phosphate, an intermediate of PPP (Table 2) further suggests increased activity of the PPP. Genes involved in ascorbate utilization are co-transcribed upstream with a transcriptional regulator (bglG) whose expression was upregulated in ΔpotABCD (Table 2). Shunting carbons to the PPP may be in response to increased demand of NADPH due to oxidative stress in the polyamine transporter-deficient mutant.

Glycolytic pathway and production of precursors for the pneumococcal capsule.

During stress, organisms modulate their gene expression to limit energy consuming processes such as CPS synthesis to preserve energy for redox systems. Gene expression profile in Δ*potABCD* indicate a limited flow of carbohydrates through the main glycolytic pathway which could be in response to stress. Expression of a sucrose operon regulator and genes involved in sucrose uptake was reduced. Expression of *malP*, which encodes an enzyme that breaks down glycogen to glucose1-phosphate and the *malXCD* operon, that encodes a maltose/maltodextrin transporter, was downregulated (Table 3). Reduced influx of sucrose, maltose, and reduced breakdown of glucose in glycolysis will deplete glycolytic intermediates in Δ*potABCD*. UDP-N-acetylglucosamine (UDP-GlcNAc) is a precursor of the three pneumococcal CPS sugar repeat units (UDP-N-acetylmannosamine (UDP-ManNAc), UDP-N-acetylgalactosamine (UDP-GalNAc) and UDP-N-acetylfucosamine (UDP-FucNAc). UDP-GlcNAc levels are expected to be low due to the elevated levels of *nagA* and *nagB*, involved in its breakdown to fructose6-phosphate (Table 3) and subsequently reduce the levels of precursors for CPS synthesis. Impaired CPS production was further apparent with the reduced expression of genes involved in the transport of N-acetylgalactosamine (Tables 3).

Table 3
The *potABCD* operon modulates central metabolism and production of precursors for the pneumococcal capsule.

Locus tag	Gene	Fold change Δ*potABCD*/TIGR4	Description
SP_2131	*bglG*	247.3	Transcriptional regulator,
SP_0100	*padR*	6.8	Transcriptional regulator
SP_1854	*galR*	3.9	LacI family transcriptional regulator
SP_2109	*malC*	-2.5	Maltodextrin ABC transporter permease
SP_2110	*malD*	-2.4	Maltodextrin ABC transporter permease
SP_2108	*malX*	-2.4	Maltose/maltodextrin-binding protein
SP_1894	*gtfA*	2.3	Sucrose phosphorylase
SP_1722	SP_1722	-51.0	PTS sucrose system EIIBCA or EIIBC
SP_0648	*bgaA*	7.0	Beta galactosidase
SP_1898	*aga*	2.2	Alpha galactosidase
SP_1721	*scrK*	-10.0	Fructokinase
SP_1725	*scrR*	-9.2	LacI family transcriptional regulator,
SP_1278	*pyrR*	-2.7	Bifunctional pyrimidine operon transcriptional regulator
SP_1724	*scrB*	-10.5	Sucrose6-phosphate hydrolase
SP_1415	*nagB*	3.2	Glucosamine-6-phosphate deaminase
SP_2056	*nagA*	2.3	N-acetylglucosamine6-phosphate deacetylase
SP_0321	SP_0321	-2.3	PTS N-acetylgalactosamine transporter subunit IIA
SP_0323	SP_0323	-2.6	PTS N-acetylgalactosamine PTS system EIIB
SP_1277	*pyrB*	-2.4	Aspartate carbamoyltransferase
SP_1014	*dapA*	-4.3	4-hydroxy-tetrahydrodipicolinate synthase
SP_1013	*asd*	-5.5	Aspartate-semialdehyde dehydrogenase

Moreover, the *pyr* operon involved in the *de novo* synthesis of pyrimidine nucleotides and *pyrR*, the regulator of this operon, were repressed (Table 3). Repression of pyrimidine biosynthetic genes will reduce UTP levels, a precursor for UDP required for the activation of UDP-sugars for CPS synthesis [24]. Expression of *asd* and *dap* involved in the synthesis of lysine, a constituent of the pneumococcal peptidoglycan layer (PG), was reduced (Table 3). The overall effect of the above gene expression changes

is reduced carbon flow through the central metabolism possibly due to stress and this will impact the production of precursors for CPS repeat unit sugars and the PG layer in the mutant. To validate RNA-Seq results, we measured the expression of selected genes using qRT-PCR (Table 4). Genes that encode for *tktC, tktN*, the ascorbate regulator (*bglG*), and the choline-binding protein *pcpA*, were upregulated, which is consistent with RNA-Seq (Table 4). Although not differentially expressed in the RNA-Seq results, polyamine synthesis genes *speE* and *speA* were upregulated in the qRT-PCR results, suggesting that polyamine synthesis could compensate for the loss of polyamine transport.

Table 4
Significant changes in Δ*potABCD* gene expression compared to TIGR4 measured by qRT-PCR.

Locus tag	Gene	Fold change Δ*potABCD*/TIGR4	Description
SP_0916	*speA*	16.9	Arginine decarboxylase
SP_0918	*speE*	14.4	Spermidine synthase
SP_2127	SP_2127	20.3	Transketolase, C-terminal subunit
SP_2128	SP_2128	27.7	Transketolase, N-terminal subunit
SP_2131	*BglG*	5.5	Transcriptional regulator
SP_2136	*pcpA*	7.2	Choline binding protein

Redox state and regulation of intracellular pH in S. pneumoniae.

Bacteria adapt to changing microenvironments by modifying metabolite levels to maintain redox homoeostasis. To gain further insight into the role of polyamine transport on the pneumococcal stress signature observed at the transcriptome level, intracellular levels of NADPH, endogenous H_2O_2, pH_i, and GSH/GSSG ratio between WT and Δ*potABCD* were compared. Our results show that deletion of the *potABCD* operon does not impact pH_i, as the pH_i of TIGR4 (7.5) and that of the mutant (7.2) were both within physiological range (Fig. 1).

There was no significant difference in the amount of NADPH produced by Δ*potABCD* (3.8 ± 0.4 µg/mg) compared to the WT (4.0 ± 0.6 µg/mg). We observed no significant difference in the amount of H_2O_2 generated by Δ*potABCD* (1 mM ± 0.05) and WT (1 mM ± 0.01). However, we observed a significant difference between the GSH/GSSG ratio of the WT (1.3 ± 0.1) and Δ*potABCD* (1.7 ± 0.1, $p \leq 0.05$). A high GSH/GSSG ratio indicates increased GSH production, for which one stimulus is oxidative stress. These results show that intracellular levels of NADPH, H_2O_2, and intracellular pH_i are not dependent on polyamine transport.

Metabolic profile of polyamine transporter deficient S. pneumoniae.

Our metabolomics results identified significant differences in the levels of several metabolites in response to *potABCD* deletion (Table 5). Levels of N-acetylglucosamine (GlcNAc) and pyruvate were reduced which

could impact CPS production in Δ*potABCD*. Increased activity of the PPP was evident by the higher levels of sedoheptulose1, 7-bisphosphate, a precursor for either erythrose4-phosphate or ribose5-phosphate. Increased galactose metabolism was shown by high levels of UDP-glucose, a precursor for glucose1-phosphate, an intermediate of glucose6-phosphate that can be channeled to PPP.

Table 5
Significant changes in metabolites in response to *potABCD* operon deletion.

Locus tag	Fold change Δ*potABCD*/TIGR4	Description
Trehalose6-phosphate	-12.1	Starch and sucrose metabolism
N-Acetylglucosamine	-2.0	Amino sugar and nucleotide sugar metabolism
Pyruvate	-1.7	Pyruvate metabolism
L-Methionine	-1.3	Cysteine and methionine metabolism
D-Gluconate	-1.2	Pentose phosphate pathway
Glutathione (GSH)	2.6	Glutathione metabolism
UDP-glucose	5.7	Galactose metabolism
Sedoheptulose1,7-bisphosphate	4.0	Galactose metabolism

The metabolome also showed reduced concentration of trehalose6-phosphate which could impact oxidative stress responses in ΔpotABCD. The concentration of glutathione was higher, which could be in response to oxidative stress in ΔpotABCD. Metabolomics results are concordant with our RNA-Seq results.

PotABCD is required for combating hydrogen peroxide and nitrosative stress.

Host defense against bacterial pathogens includes generation of ROS such as superoxide anions (O_2•⁻), H_2O_2 and hydroxyl radicals (OH•) as well as reactive nitrogen species (RNS). To further corroborate the stress signature observed at the transcriptome and metabolome levels, we compared the susceptibility of TIGR4 and Δ*potABCD* to unstable oxygen and nitrogen radicals. Our results show that Δ*potABCD* is more susceptible to hydrogen peroxide stress compared to the WT. When cultured in the presence of low concentrations of exogenous hydrogen peroxide (0.5, 0.75 and 1 mM), there was no significant effect on the growth of WT and Δ*potABCD* at 15- and 30 min post exposure (data not shown). However, in the presence of 2.5 mM H_2O_2, viability of Δ*potABCD* was reduced by (54%) relative to WT at 15 min post exposure but was restored by ~ 25% in the complement pABG5-*potABCD* strain or with ¼MIC (2.5 mM) cadaverine supplementation (Fig. 2). Polyamine supplementation was done on Δ*potABCD* cultured in chemically defined growth medium (CDM) which lacks synthesized polyamines.

Compared to WT, Δ*potABCD* was significantly more susceptible to *S*-nitrosoglutathione (*GSNO*) that generates RNS. Exposure to *GSNO* for 60 min at a concentration of 2.5 mM resulted in a significant reduction in the percentage survival of Δ*potABCD* that ranged between 32% at 15- min and 73% at 60 min post exposure compared to the WT (0% at 15 min and 10% at 60 min post exposure). There was no significant difference in the survival of the complement pABG5-*potABCD* strain or supplementation with polyamines in the presence of *GSNO* (Figure 3). These results suggest that Δ*potABCD* is more susceptible to H_2O_2 and nitrosative stress than WT. Data with pABG5-*potABCD* complement or polyamine supplementation indicates that impact of impaired polyamine transport could be specific to the type of stress.

Discussion

Findings in this study show that deficiency of polyamine transport impairs pneumococcal stress responses and disrupts CPS and PG synthesis (Fig. 4). This study also shows that the *potABCD* operon is involved in hydrogen peroxide and nitrosative stress responses in pneumococci. Polyamines contribute to cellular homeostasis by scavenging reactive radicals or balance intracellular pH through the consumption of a proton during their synthesis via the decarboxylation of amino acids [25, 26]. Therefore, reduced intracellular polyamine levels reported in Ayoola et al. [15] and decreased expression of some genes involved in redox balance in the current study, could render Δ*potABCD* susceptible to stress. In addition, polyamines regulate transcription of several genes including those involved in oxidative stress responses. Downregulation of expression of *treR* that impact the levels of trehalose a scavenger of ROS and the impaired DNA repair system could make the mutant sensitive to stress. The damage caused by H_2O_2 can be amplified via the Fenton reaction with the generation of hydroxyl radicals, the primary cause of damage to biomolecules such as DNA [27]. Therefore, increased expression of the iron transporter could aggravate the effects of oxidative stress and impair pneumococcal survival *in vivo*, as it moves through different host niches.

In response to the stress caused by polyamine transport deficiency, Δ*potABCD* triggered other known stress response systems to restore the redox status. Acquisition of P_i and manganese is essential for normal growth, virulence, and oxidative stress responses in many pathogenic bacteria [17, 22, 28]. The PPP is often upregulated as a quick cellular response to meet NADPH demands to combat oxidative stress [23]. The ADS produces ammonia (NH_3) that protect cells against acid stress and a molecule of ATP for basal cellular functions during stress [29, 30]. Reduced glutathione and glutathione metabolism play a significant role during oxidative stress in many organisms [31–33]. Therefore, increased expression of genes involved in cation influx, PPP, the ADS, and a high GSH/GSSG ratio could be in response to stress in Δ*potABCD.* [17, 34]. Upregulation of the ADS could explain the observation that Δ*potABCD* can maintain pH_i in the physiological range. The polyamine modulon which represent genes whose expression is regulated by polyamines is well described in *Escherichia coli* and includes genes involved in cell proliferation, biofilm formation, and detoxification of ROS [35]. Our results show that deficiency of the polyamine transporter affected the transcript level of several regulators, and thus

indirectly altering genes controlled by these regulators. Interestingly, we observed that some polyamine transporter responsive genes are also part of the CcpA regulatory network, for example genes involved in stress responses, amino acid synthesis, and carbohydrate metabolism [36, 37]. These results suggest that the intersection of polyamine metabolism and CcpA regulatory network is needed for *in vivo* fitness. These results warrant future studies to identify mechanisms of co-regulation of polyamine metabolism and other transcriptional regulators that impact pneumococcal virulence.

Furthermore, upregulation of the Leloir and the tagatose pathways that produce PPP intermediates, and transketolase, a key enzyme in PPP, further suggest decreased carbon flow through glycolysis, supported by decreased pyruvate levels in *ΔpotABCD*. Decreased glycolysis could result in reduced acetyl-CoA, a precursor for UDP-GlcNAc, and a donor for the three N-acetylated sugars at the intersection of CPS and PG repeat unit biosynthesis [38, 39]. However, upregulation of genes involved in the Leloir pathway in Δ*potABCD* is contrary to what was observed in Δ*speA* [15]. Deletion of arginine decarboxylase (*speA*) resulted in downregulation of genes of the Leloir pathway, implicating a role for polyamine synthesis in the regulation of this pathway. Arginine decarboxylase in Δ*potABCD* could result in the upregulation of the Leloir pathway which warrants further investigation. The PPP generates ribulose5-phosphate which can either be used for nucleotide synthesis or converted to sedoheptulose1, 7-bisphosphate, a precursor for erythrose4-phosphate and G3P. High levels of sedoheptulose1, 7-bisphosphate suggest that Δ*potABCD* promotes PPP activity possibly to increase production of NADPH levels required in redox systems. Downregulation of the *pyr* operon, responsible for the interconversion of uracil and uridine monophosphate (UMP), could impact UDP production necessary for UDP-sugar repeat unit synthesis and further impair CPS biosynthesis. Results from this study and our previous report [15] demonstrate that polyamine mediated CPS and PG regulation is dependent on both polyamine transport and synthesis. Reduction of CPS precursors could explain the un-encapsulated phenotype and attenuation of Δ*potABCD* in murine models of colonization, pneumonia, and sepsis [10, 15].

Hydrogen peroxide produced by the pneumococcus is essential for its pathogenesis and protection against other common respiratory tract inhabitants. H_2O_2 is cytotoxic to host cells, causes apoptosis in respiratory epithelial cells, and promotes colonization of the upper respiratory tract [40]. Therefore, pneumococci must adapt to survive the high levels of H_2O_2 produced via the pyruvate oxidase system. Despite a high GSH/GSSG ratio, maintenance of NADPH levels and upregulation of several genes involved in oxidative stress responses, Δ*potABCD* was more susceptible to hydrogen peroxide and nitrosative stress comparable to the WT. The increased susceptibility to H_2O_2 cannot be attributed to increased intracellular H_2O_2 levels in Δ*potABCD* since they were comparable to that produced by WT. These results suggest that polyamines could be essential for the regulation of up/down stream functions of pneumococcal oxidative stress responses which warrants further investigation. These results are consistent with the known roles of polyamines in other bacterial pathogens [8]. Putrescine and spermidine protect cells from ROS by increasing expression of genes that code for free radical scavengers [41, 42]. Polyamine synthesis [43] or transport genes are upregulated [9] in response to H_2O_2 stress. Cadaverine protects *Salmonella typhimurium* and *E. coli* against nitrosative and acid stress [44,

45]. Pneumococci increase transcription of the substrate binding protein (*potD*) of the polyamine transporter in response to oxidative and thermal stress and during murine bacteremia [9]. We also reported that *speA*, a gene that encodes an arginine decarboxylase, regulates pneumococcal nitrosative, H_2O_2 and superoxide stress responses (manuscript under review). These results show that polyamine uptake from the environment may potentially help pneumococci to survive various host microenvironments. However, only supplementation with 2.5 mM cadaverine restored mutant viability in the presence of H_2O_2 but not *GSNO*. These results indicate that providing the transport function in trans (pABG5-*potABCD* complement) or by exogenous polyamine supplementation has varying effects on the viability of Δ*potABCD* that is dependent on the type of stress and the type and concentration of polyamines.

In summary, polyamine transport is essential for pneumococcal stress responses and a dysregulation of these responses impacts the synthesis of CPS and PG. Through horizontal gene transfer, a non-virulent pneumococci can become encapsulated and virulent during coinfections in the host [46] which confounds management strategies. Therefore, gaining insights into virulence mechanisms that are capsule independent but modulate capsule production, like polyamine metabolism, present a novel avenue for exploring new vaccine and therapeutic interventions against this deadly pathogen. Polyamine transport systems are conserved across pneumococcal serotypes and are a promising therapeutic avenue due to their immunogenic potential [12, 14]. Future studies focusing on uncovering the interconnected network of pneumococcal polyamine redox homeostasis, CPS and PG synthesis will contribute towards deconvolution of the complex regulatory networks that impact stress responses and pneumococcal adaptation *in vivo*.

Materials And Methods

Bacterial strains and growth conditions.

S. pneumoniae serotype 4 strain TIGR4 [47], Δ*potABCD* [11], and the complement strain (pABG5-*potABCD*) [15] were used in this study. All strains were grown in either chemically defined medium (CDM) [48] or Todd- Hewitt broth supplemented with 0.5% yeast extract (THY) or on 5% sheep blood agar plates (BAP) in 5% CO_2 at 37°C. All assays were performed in triplicate in three independent experiments.

RNA Sequencing.

Total RNA was isolated and purified from mid-log phase cultures (OD_{600} 0.4) of TIGR4 and Δ*potABCD* (n = 4) grown in THY (a complete medium that mimics nutrients in the host milieu) using the RNeasy® Mini Kit (Qiagen, Valencia, CA, USA). RNA quality was checked with an Agilent 2100 Bioanalyzer (Agilent Technologies, Santa Clara, CA, USA). RNA-Seq analysis was performed as described earlier [15]. Briefly, libraries for RNA-Seq were prepared with the KAPA RNA Hyper Kit with RiboErase (KAPA Biosystem, Wilmington, MA, USA) with 5 µg RNA as input. The concentration and quality of libraries were determined by the Qubit ds DNA HS Assay Kit (Life Technologies, Carlsbad, CA, USA) and Agilent Tapestation (Agilent

Technologies, Santa Clara, CA, USA). Sequencing was done on Illumina Hiseq 3000, the quality of the data was checked with Illumina SAV and de-multiplexing was performed with Illumina Bcl2fastq2 v 2.17. Removal of failed reads, mapping of the short sequence reads to the TIGR4 reference genome, and identification of differentially expressed genes were performed with CLC Genomic Workbench 20.0.3 (Qiagen, Valencia, CA, USA).

Paired end reads of both WT and Δ*potABCD* were mapped to the TIGR4 genome using CLC proprietary read mapper and read counts were estimated by EM estimation algorithm [49] and DEGs were identified based on the fold change generated by the edgeR algorithm. Changes in gene expression with a fold change of ± 1.3 at a false discovery rate (FDR) of ≤ 0.05 were considered significant. Functions and pathways represented by DEGs were identified utilizing multiple bioinformatics resources such as MetaCyc [50], Gene Ontology [51], KEGG [52], UniProt [53], and STRING [54]. RNA-Seq raw data and metadata are available at NCBI GEO with the accession number XXXXXXX.

Quantitative real time PCR.

To validate RNA-Seq results, we measured expression of selected genes by quantitative reverse transcription PCR (qRT-PCR). The primers used for qRT-PCR are listed in supplementary material (Supp. Table 1). All primers were validated by performing a melt curve analysis with SYBR Green (Thermo Fisher Scientific Waltham, MA, USA). In brief, total RNA was purified from mid-log phase cultures (OD_{600} 0.4) of TIGR4 and Δ*potABCD* grown in THY (n = 3). Purified RNA (7.5 ng/reaction) was reverse-transcribed into cDNA and PCR was performed using the SuperScript III Platinum SYBR Green One-Step qRT-PCR Kit (Thermo Fisher Scientific, Waltham, MA, USA) as previously described [55]. Relative quantification of gene expression was determined by the Stratagene Mx3005P qPCR System (Agilent, Santa Clara, CA, USA). Expression of selected genes was normalized to the expression of *gapDH* and fold changes determined by the comparative C_T method.

Measurement of intracellular pH.

The intracellular pH (pH_i) was determined based on the method described by Clementi et al., [56] with slight modifications. Briefly, mid-log phase cultures (OD_{600} 0.4) of TIGR4 and Δ*potABCD* grown in THY (n = 3) were collected by centrifugation, washed, and suspended in phosphate buffered saline (PBS). Cells (10^8 CFU/mL) were loaded with 5 mM BCECF/AM dye (Millipore-Sigma, St. Louis, MO, USA) and incubated for 30 min at 30°C in the dark. Cells were then pelleted, washed, and reenergized with 10 mM glucose in PBS. To obtain the *in vivo* calibration curve for each strain, 400 µL of energized cells were pelleted and suspended in potassium buffers ranging from pH 6.5 to 8.0. Nigericin (1 mM) (Thermo Fisher Scientific, Waltham, MA, USA) was added to the cells (to equilibrate the pH_i of the cells to the pH of the surrounding buffer) and incubated at 37°C for 5 min. Fluorescence was then measured by a Synergy H1 plate reader (BioTek, Winooski, VT, USA), and a calibration curve was obtained by plotting fluorescence against the pH of the buffers. To measure the pH of individual samples, 200 µL (10^8 CFU/mL) of the loaded and energized cells was added to the wells of a 96-well plate in duplicate and fluorescence

detected using a plate reader for 5 min. 10 μM carbonyl cyanide 3-chlorophenylhydrazone (CCCP) was added to one well (to serve as control) and the reading taken for another 5 min. CCCP is a protonophore that uncouples proton motive force and causes a rapid decrease in pH_i (Millipore-Sigma, St. Louis, MO, USA). Nigericin was added to both CCCP-treated control and untreated sample (to a final concentration of 1 mM) to equilibrate the pH_i to the pH of the buffer and fluorescence was read for an additional 5 min. Fluorescence was calculated and the pH_i was interpolated from the calibration curve.

Measurement of intracellular NADPH.

The intracellular concentration of NADPH was determined using the NADP/NADPH Assay Kit (Abcam, Cambridge, MA, USA). Mid-log phase cultures (n = 3) were harvested at 5,000 × g for 10 min at 4°C, suspended in PBS and transferred to beadbeater tubes (MP Biomedicals, Irvine, CA, USA). Cell suspensions were lysed with a FastPrep-24™ Classic benchtop homogenizer (MP Biomedicals, Irvine, CA, USA) and centrifuged at 6,000 × g for 5 min at 4°C. The cells were processed according to the manufacturer's instructions. NADPH concentrations were determined with a SpectraMax® M5 multi-mode microplate reader (Molecular Devices, Sunnyvale, CA, USA). The concentration of the protein extracts was determined with the Pierce BCA Protein Assay Kit (Thermo Fisher Scientific, Waltham, MA, USA) and used to normalize NADPH concentrations.

Measurement of intracellular glutathione.

The ratios of reduced (GSH) to oxidized (GSSG) intracellular glutathione concentrations were determined using the GSH/GSSG-Glo™ Assay Kit (Promega, Madison, WI, USA). The cells were processed, and protein concentration determined as was done for NADPH quantification above. Luminescence was measured with a Cytation™ 5 cell imaging multi-mode reader (BioTek, Winooski, VT, USA) and used to calculate glutathione concentrations. The concentration of the protein extracts was determined with the Pierce BCA Protein Assay Kit (Thermo Fisher Scientific, Waltham, MA, USA) and used to normalize glutathione concentrations. GSH/GSSG (reduced/oxidized glutathione) ratios were calculated from the normalized glutathione concentrations according to the manufacturer's instructions.

UPLC–HRMS untargeted metabolomics.

Approximately 10^9 CFU/mL of cells from mid-log phase cultures of TIGR4 and Δ*potABCD* grown in THY (n = 5) were transferred onto a 0.2 μm Whatman polycarbonate membrane by vacuum filtration. The membranes were snap-frozen in liquid nitrogen and stored at − 80°C. Metabolites were extracted from bacteria on the membranes with extraction solvent (40:40:20 methanol, acetonitrile, and water with 0.1% formic acid) at 4°C (16). The extracts were transferred to 2.0 mL tubes, centrifuged for 5 min (16,100 × g) at 4°C and the supernatant transferred to new 2.0 mL tubes. Tubes containing ~1.7 mL of the total supernatant were dried under a stream of N_2 and solid residue was suspended in 300 μL of sterile water and transferred to autosampler vials for mass spectrometric analysis. A 10 μL aliquot was injected through a Synergi 2.5-micron reverse-phase Hydro-RP 100, 100 × 2.00 mM LC column (Phenomenex, Torrance, CA, USA) kept at 25°C. The eluent was introduced into the MS via an electrospray ionization

source conjoined to an Exactive™ Plus Orbitrap Mass Spectrometer (Thermo Scientific, Waltham, MA, USA) through a 0.1 mm internal diameter fused silica capillary tube. The mass spectrometer was run in full scan mode with negative ionization mode with a window from 85 to 1000 *m/z* with a method adapted from [57]. Samples were run with a spray voltage of 3 kV. The nitrogen sheath gas was set to a flow rate of 10 psi with a capillary temperature of 320°C. Automatic gain control target was set to 3e6. The samples were analyzed with a resolution of 140,000 and a scan window of 85–800 *m/z* from 0 to 9 min and 110–1000 m/z from 9 to 25 min. Files generated by Xcalibur (RAW) were converted to the open source mzML format [49] via the open source msconvert software as part of the ProteoWizard package [49]. Maven (mzroll) software, Princeton University [58, 59] was used to automatically correct the total ion chromatograms based on the retention times for each sample [58, 59]. Metabolites were manually identified and integrated using known masses (± 5 ppm mass tolerance) and retention times (1 ≤ 1.5 min). Unknown peaks were automatically selected via Maven's automated peak detection algorithms. A database of 275 metabolites verified using exact *m/z* and known retention times, expanded from the original database [57] was used. The statistical analysis on metabolite peak intensity post CFU normalization was done by MetaboAnalyst 4.0 [60]. Quantile normalization which is highly efficient in normalizing metabolite variations from mass spectrometry [61] was used to normalize the data. Significant differences in metabolite peak intensity between Δ*potABCD* and TIGR4 were identified by a T-test at an adjusted FDR of ≤ 0.05. .

Hydrogen peroxide production.

H_2O_2 generated from mid-log phase cultures of TIGR4 and Δ*potABCD* (n = 3) was compared using a quantitative peroxide assay (Pierce, Thermo Fisher Scientific Waltham, MA, USA). Briefly, 1 mL of bacterial culture (10^8 CFU/mL) grown in THY was centrifuged at 4 C for 2 min at 10,000 x g and the supernatant filtered with a 0.22 µm filter. The concentration of H_2O_2 was measured in the filtrate following the manufacturer's instructions.

Hydrogen peroxide survival.

Mid-log phase cultures of TIGR4, Δ*potABCD* and the complement pABG5-*potABCD* strain grown in either THY or CDM (OD_{600} 0.4–0.5) were centrifuged at 10,000 x g for 2 min and suspended in PBS. The cells (10^8 CFU/mL) (in 1 mL PBS) were then supplemented with final concentrations of hydrogen peroxide 2.5 mM and incubated at 37°C with 5% CO_2 for 15 min. CDM is devoid of polyamines but has the amino acid precursors for polyamine synthesis. To determine the effects of polyamines on pneumococcal H_2O_2 stress, Δ*potABCD* challenged with 2.5 mM H_2O_2, was supplemented with cadaverine, putrescine or spermidine (½MIC, ¼MIC, ⅛MIC) and incubated for 15 min. MICs for cadaverine, spermidine or putrescine are 10.0, 4.8 and 5.7 mM, respectively. Control reactions had untreated bacteria, and CFUs were determined by serial dilution in PBS and plating on BAP. Results from three independent experiments were expressed as percent survival of treated bacteria relative to the untreated bacteria.

S -nitrosoglutathione susceptibility.

Mid-log phase cultures of TIGR4, Δ*potABCD* and the complement pABG5-*potABCD* strain grown in CDM were centrifuged at 10,000 x g for 2 min and cells suspended in PBS. The cells (10^7 CFU/mL) in 100 µl were supplemented with a final concentration of 2.5 mM *GSNO* (Sigma-Aldrich, Israel), a nitric oxide producer, and incubated at 37°C in 5% CO_2 for 60 min. In addition, Δ*potABCD* challenged with 2.5 mM *GSNO* was supplemented with cadaverine, putrescine or spermidine (½MIC, ¼MIC, ⅛MIC). Control reactions had untreated bacteria, and CFUs were determined by serial dilution in PBS and plating on BAP every after 15 min. Results from three independent experiments were expressed as percent survival of treated bacteria relative to the untreated bacteria.

Statistical analysis.

Significant differences between the susceptibility of TIGR4, Δ*potABCD* and the complement pABG5-*potABCD* strain to the different stressors, changes in pH_i, production of endogenous H_2O_2, levels of NADPH and GSH/GSSG ratio, as well as changes in gene expression measured by qRT-PCR were determined by a Student's T-test at $p \leq 0.05$.

Declarations

Authors and contributors.

B.N. conceived, designed, and supervised the experiments. M.F.N performed the experiments and drafted the manuscript. L.A.S., M.M. and M.B.A. performed the experiments. B.N. and E.S. contributed to the final draft. All authors approved the final version of the manuscript.

Conflicts of interest.

The authors declare no conflict of interest in this work.

Funding information.

Grant: #P20GM103646 (Center for Biomedical Research Excellence in Pathogen Host Interactions) from the National Institute for General Medical Sciences.

Acknowledgements.

This work was supported by grant #P20GM103646 (Center for Biomedical Research Excellence in Pathogen Host Interactions) from the National Institute for General Medical Sciences.

Metabolomics extraction and mass spectrometric analyses were performed at the Biological and Small Molecule Mass Spectrometry Core, University of Tennessee, Knoxville, Knoxville, TN, United States, with the assistance of Dr. Shawn R. Campagna, Dr. Hector F. Castro, and Joshua B. Powers.

References

1. Katherine L O'Brien, L.J.W., James P Watt, Emily Henkle, Maria Deloria-Knoll, Natalie McCall, Ellen Lee, Kim Mulholland, Orin S Levine, and Thomas Cherian, *Burden of disease caused by Streptococcus pneumoniae in children younger than 5 years: global estimates.* Lancet, 2009 **374**: p. 893–902.
2. Dion CF, A.J., *Streptococcus Pneumoniae. .* In: StatPearls [Internet]. Treasure Island (FL): StatPearls 2020.
3. DM., M., *Infections caused by Streptococcus pneumoniae: clinical spectrum, pathogenesis, immunity, and treatment. .* Clin Infect Dis., 1992. **14**(4): p. 801-7.
4. Berical, A.C., Harris, D., Dela Cruz, C. S., Possick, J. D., *Pneumococcal Vaccination Strategies. An Update and Perspective.* Ann Am Thorac Soc, 2016. **13**(6): p. 933-44.
5. Balsells, E.G., L. Nair, H. Kyaw, M. H., *Serotype distribution of Streptococcus pneumoniae causing invasive disease in children in the post-PCV era: A systematic review and meta-analysis.* PLoS One, 2017. **12**(5): p. e0177113.
6. Cherazard R, E.M., Doan TL, Salim T, Bharti S, Smith MA., *Antimicrobial Resistant Streptococcus pneumoniae: Prevalence, Mechanisms, and Clinical Implications. .* Am J Ther. , 2017. **24**(3): p. e361-e369. .
7. Igarashi, K.a.K., K., *Characteristics of cellular polyamine transport in prokaryotes and eukaryotes.* Plant Physiol Biochem, 2010. **48**(7): p. 506-12.
8. Shah, P. and E. Swiatlo, *A multifaceted role for polyamines in bacterial pathogens.* Mol Microbiol, 2008. **68**(1): p. 4-16.
9. Shah, P., D.G. Romero, and E. Swiatlo, *Role of polyamine transport in Streptococcus pneumoniae response to physiological stress and murine septicemia.* Microb Pathog, 2008. **45**(3): p. 167-72.
10. Shah, P.N., B. Swiatlo, E.,Ma, Y. Pendarvis, K., *Polyamine biosynthesis and transport mechanisms are crucial for fitness and pathogenesis of Streptococcus pneumoniae.* Microbiology, 2011. **157**(Pt 2): p. 504-15.
11. Rai, A.N., Thornton, J. A., Stokes, J., Sunesara, I., Swiatlo, E., Nanduri, B., *Polyamine transporter in Streptococcus pneumoniae is essential for evading early innate immune responses in pneumococcal pneumonia.* Sci Rep, 2016. **6**: p. 26964.
12. Converso, T.R., Goulart, C., Rodriguez, D., Darrieux, M., Leite, L. C., *Systemic immunization with rPotD reduces Streptococcus pneumoniae nasopharyngeal colonization in mice.* Vaccine, 2017. **35**(1): p. 149-155.
13. Shah, P. and E. Swiatlo, *Immunization with polyamine transport protein PotD protects mice against systemic infection with Streptococcus pneumoniae.* Infect Immun, 2006. **74**(10): p. 5888-92.
14. Shah P, B.D., King J, Hale Y, Swiatlo E, *Mucosal immunization with polyamine transport protein D (PotD) protects mice against nasopharyngeal colonization with Streptococcus pneumoniae.* Exp Biol Med 2009 **234**(4): p. 403-9.
15. Ayoola, M.B.S., Leslie A. Nakamya, Mary F. Thornton, Justin A. Swiatlo, Edwin Nanduri, Bindu, *Polyamine Synthesis Effects Capsule Expression by Reduction of Precursors in Streptococcus*

pneumoniae. Frontiers in Microbiology, 2019. **10**.

16. Rhee, H.J., E.J. Kim, and J.K. Lee, *Physiological polyamines: simple primordial stress molecules.* J Cell Mol Med, 2007. **11**(4): p. 685-703.
17. Alejandro Gómez-Mejia, G.G., Stephanie Hirschmann, Viktor Kluger, Hermann Rath, Sebastian Böhm, Franziska Voss, Niamatullah Kakar, Lothar Petruschka, Uwe Völke, Reinhold Brückner, Ulrike Mäder and Sven Hammerschmidt, *Pneumococcal metabolic adaptation and colonization is regulated by 1thetwo-component regulatory system 08.* msphere, 2018. **3** (3).
18. Kwon HY, K.E., Tran TD, Pyo SN, Rhee DK., *Reduction-sensitive and cysteine residue-mediated Streptococcus pneumoniae HrcA oligomerization in vitro. .* Mol Cells., 2009. **27**: p. 149-57.
19. Marc Torrent, G.C., Natalia S. de Groot, Arthur Wuster, M. Madan Babu, *Cells alter their tRNA abundance to selectively regulate protein synthesis during stress conditions.* Sci. Signal, 2018. **11**.
20. Carvalho, S.M.K., T. G. Manzoor, I. Caldas, J. Vinga, S. Martinussen, J. Saraiva, L. M. Kuipers, O. P. Neves, A. R, *Interplay Between Capsule Expression and Uracil Metabolism in Streptococcus pneumoniae D39.* Front Microbiol, 2018. **9**: p. 321.
21. Crawford, M.A., Henard,Calvin A., Tapscott,Timothy, Porwollik,Steffen, McClelland,Michael, Vázquez-Torres,Andrés, *DksA-Dependent Transcriptional Regulation in Salmonella Experiencing Nitrosative Stress.* Frontiers in Microbiology, 2016. **7**(444).
22. Ogunniyi, A.D., Mahdi, L. K., Jennings, M. P., McEwan, A. G., McDevitt, C. A., Van der Hoek, M. B., Bagley, C. J., Hoffmann, P., Gould, K. A., Paton, J. C., *Central role of manganese in regulation of stress responses, physiology, and metabolism in Streptococcus pneumoniae.* J Bacteriol, 2010. **192**(17): p. 4489-97.
23. Stincone, A., Alessandro Prigione, Thorsten Cramer, Mirjam M. C., Wamelink, Kate Campbell , Eric Cheung, Viridiana Olin-Sandoval, Nana-Maria Grüning, Antje Krüger, Mohammad Tauqeer Alam, Markus A. Keller, Michael Breitenbach, Kevin M. Brindle, Joshua D., Rabinowitz, Markus Ralser, *The return of metabolism: biochemistry and physiology of the pentose phosphate pathway.* Biol Rev Camb Philos Soc 2015 **90**(3): p. 927–963.
24. Kilstrup, M., Hammer, K., Ruhdal Jensen, P., Martinussen, J., *Nucleotide metabolism and its control in lactic acid bacteria.* FEMS Microbiol Rev, 2005. **29**(3): p. 555-90.
25. Winterhoff N, G.R., Gruening P, Rohde M, Kalisz H, Smith HE, Valentin-Weigand P., *Identification and characterization of two temperature-induced surface-associated proteins of Streptococcus suis with high homologies to members of the Arginine Deiminase system of Streptococcus pyogenes. .* J Bacteriol. , 2002. **184**(24): p. 6768-76.
26. Cabiscol, E.T.J.R.J., *Oxidative stress in bacteria and protein damage by reactive oxygen species.* Int Microbiol., 2000 **3**(1): p. 3-8.
27. Imlay, J.A., *Iron-sulphur clusters and the problem with oxygen.* Molecular Microbiology 2006. **59**(4): p. 1073–1082.
28. Caroline, M.G., Jacob E. Choby, Lillian J. Juttukonda, William N. Beavers, Andy Weiss, Victor J. Torres, Eric P. Skaar, *Manganese Detoxification by MntE Is Critical for Resistance to Oxidative Stress*

and Virulence of Staphylococcus aureus. Molecular Biology, 2019 **10** (1).

29. Patil MD, R.V., Bihade UR, Banerjee UC., *Purification and characterization of arginine deiminase from Pseudomonas putida: Structural insights of the differential affinities of l-arginine analogues. .* J Biosci Bioeng. , 2019. **27**(2): p. 129-137.
30. Nicholas S. Jakubovics, J.C.R., Derek S. Samarian, Ethan Kolderman, Sufian A. Yassin, Deepti Bettampadi, Matthew Bashton and Alexander H. Rickard, *Critical roles of arginine in growth and biofilm development by Streptococcus gordonii.* Molecular Microbiology 2015. **97**(2): p. 281–300.
31. Potter, A.J., C. Trappetti, and J.C. Paton, *Streptococcus pneumoniae uses glutathione to defend against oxidative stress and metal ion toxicity.* J Bacteriol, 2012. **194**(22): p. 6248-54.
32. John P. Lisher, H.-C.T.T., Smirla Ramos-Montañez, Kristy L. Hentchel, Julia E. Martin, Jonathan C. Trinidad, Malcolm E. Winkler, David P. Giedroca,, *Biological and Chemical Adaptation to Endogenous Hydrogen Peroxide Production in Streptococcus pneumoniae D39.* Molecular Biology and Physiology, 2017. **2** (1): p. e00291-16.
33. Li Y, H.J., Abee T, Molenaar D., *Glutathione protects Lactococcus lactis against oxidative stress.* Appl Environ Microbiol, 2003 **69**(105739-45).
34. Carmel-Harel, O.a.S., G., *Roles of the glutathione- and thioredoxin-dependent reduction systems in the Escherichia coli and Saccharomyces cerevisiae responses to oxidative stress.* Annu Rev Microbiol, 2000. **54**: p. 439-61.
35. Kashiwagi, K.I.a.K., *Effects of polyamines on protein synthesis and growth of Escherichia coli. .* J. Biol. Chem. , 2018. **293**(48): p. 18702–18709.
36. Paluscio, E., M.E. Watson, and M.G. Caparon, *CcpA Coordinates Growth/Damage Balance for Streptococcus pyogenes Pathogenesis.* Scientific Reports, 2018. **8**(1).
37. Antunes, A., Camiade, Emilie, Monot, Marc, Courtois, Emmanuelle, Barbut, Frédéric, Sernova, Natalia V., Rodionov, Dmitry A., Martin-Verstraete, Isabelle, Dupuy, Bruno, *Global transcriptional control by glucose and carbon regulator CcpA in Clostridium difficile.* Nucleic Acids Research, 2012. **40**(21): p. 10701-10718.
38. Emily J. Kay, L.E.Y., Vanessa S. Terra, Jon Cuccuiand Brendan W. Wren. , *Recombinant expression of Streptococcus pneumoniae capsular polysaccharides in Escherichia coli.* Open Biol., 2016. **13**(6): p. 150243.
39. Chen, L.L.H., D. L. Zhai, Y. F. Wang, J. H. Wang, Y. F. Chen, M., *Characterization and Mutational Analysis of Two UDP-Galactose 4-Epimerases in Streptococcus pneumoniae TIGR4.* Biochemistry (Mosc), 2018. **83**(1): p. 37-44.
40. Rai, P., et al., *Streptococcus pneumoniae secretes hydrogen peroxide leading to DNA damage and apoptosis in lung cells.* Proc Natl Acad Sci U S A, 2015. **112**(26): p. E3421-30.
41. Tkachenko, A.G., Akhova, Anna V., Shumkov, Mikhail S., Nesterova, Larisa Yu, *Polyamines reduce oxidative stress in Escherichia coli cells exposed to bactericidal antibiotics.* Research in Microbiology, 2012. **163**(2): p. 83-91.

42. Elisa Cabiscol, J.T.a.J.R., *Oxidative stress in bacteria and protein damage by reactive oxygen species.* International Microbiology · 2000. **3**: p. 3–8.
43. Chattopadhyay, C.W.T.a.H.T., *Polyamines protect Escherichia coli cells from the toxic effect of oxygen.* Biochemistry, 2003. **100** (5): p. 2261–2265.
44. Espinel, I.C., Guerra, P. R., Jelsbak, L., *Multiple roles of putrescine and spermidine in stress resistance and virulence of Salmonella enterica serovar Typhimurium.* Microb Pathog, 2016. **95**: p. 117-123.
45. Bower, J.M. and M.A. Mulvey, *Polyamine-mediated resistance of uropathogenic Escherichia coli to nitrosative stress.* J Bacteriol, 2006. **188**(3): p. 928-33.
46. Moon H. Nahm, T.B., Mogens Kilian, Jiri Vlach, Carlos J. Orihuela, Jamil S. Saad, and Feroze Ganaie., *Pneumococci Can Become Virulent by Acquiring a New Capsule From Oral Streptococci.* The Journal of Infectious Diseases, 2020. **6;222**(3): p. 372-380.
47. Herve Tettelin, K.E.N., Ian T. Paulsen, Jonathan A. Eisen, Timothy D. Read, Scott Peterson John Heidelberg, Robert T. DeBoy, Daniel H. Haft, Robert J. Dodson, A. Scott Durkin, Michelle Gwinn, James F. Kolonay, William C. Nelson, Jeremy D. Peterson, Lowell A. Umayam, Owen White, Steven L. Salzberg, Matthew R. Lewis, Diana Radune, Erik Holtzapple, Hoda Khouri, Alex M. Wolf, Terry R. Utterback, Cheryl L. Hansen, Lisa A. McDonald, Tamara V. Feldblyum, Samuel Angiuoli, Tanja Dickinson, Erin K. Hickey, Ingeborg E. Holt, Brendan J. Loftus, Fan Yang, Hamilton O. Smith, J. Craig Venter, Brian A. Dougherty, Donald A. Morrison, Susan K. Hollingshead, Claire M. Fraser, *Complete Genome Sequence of a Virulent Isolate of Streptococcus pneumoniae.* Science, 2001 **293**.
48. Esther Texeira, J.C., Analía Ríal, Jose A. Chabalgoity, Norma Suárez, *A new chemically defined medium for cultivation of Streptococcus pneumoniae Serotype 1.* Journal of Biotech Research, 2015. **6**: p. 54-62.
49. Lennart Martens, M.C., Marc Sturm, Darren Kessner, Fredrik Levander, Jim Shofstahl, Wilfred H. Tang, Andreas Ro¨mpp, Steffen Neumann, Angel D. Pizarro, Luisa Montecchi-Palazzi, Natalie Tasman, Mike Coleman, Florian Reisinger, Puneet Souda, Henning Hermjakob, Pierre-Alain Binz, and Eric W. Deutschh., *mzML—a Community Standard for Mass Spectrometry Data.* Molecular & Cellular Proteomics 2011. **10**(1).
50. Keseler, I.M.M., A. Santos-Zavaleta, A. Billington, R. Bonavides-Martinez, C. Caspi, R. Fulcher, C. Gama-Castro, S. Kothari, A. Krummenacker, M. Latendresse, M. Muniz-Rascado, L. Ong, Q. Paley, S. Peralta-Gil, M. Subhraveti, P. Velazquez-Ramirez, D. A. Weaver, D. and J.P. Collado-Vides, I. Karp, P. D., *The EcoCyc database: reflecting new knowledge about Escherichia coli K-12.* Nucleic Acids Res, 2017. **45**(D1): p. D543-D550.
51. The Gene Ontology, C., *Expansion of the Gene Ontology knowledgebase and resources.* Nucleic Acids Res, 2017. **45**(D1): p. D331-D338.
52. Kanehisa, M.G., S. Sato, Y. Furumichi, M. Tanabe, M., *KEGG for integration and interpretation of large-scale molecular data sets.* Nucleic Acids Research, 2011. **40**(D1): p. D109-D114.
53. UniProt Consortium, T., *UniProt: the universal protein knowledgebase.* Nucleic Acids Res, 2018. **46**(5): p. 2699.

54. Szklarczyk, D.G., A. L. Lyon, D. Junge, A. Wyder, S. Huerta-Cepas, J. Simonovic, M. Doncheva, N. T. Morris, J. H. Bork, P. Jensen, L. J. Mering, C. V., *STRING v11: protein-protein association networks with increased coverage, supporting functional discovery in genome-wide experimental datasets.* Nucleic Acids Res, 2019. **47**(D1): p. D607-D613.
55. Qian WJ, J.J., Camp DG 2nd, Monroe ME, Moore RJ, Gritsenko MA, Calvano SE, Lowry SF, Xiao W, Moldawer LL, Davis RW, Tompkins RG, Smith RD. , *Comparative proteome analyses of human plasma following in vivo lipopolysaccharide administration using multidimensional separations coupled with tandem mass spectrometry.* Proteomics, 2005 **5**(2): p. 572-8.
56. Clementi, E.A.M., L. R. Roche-Hakansson, H. Hakansson, A. P. , *Monitoring changes in membrane polarity, membrane integrity, and intracellular ion concentrations in Streptococcus pneumoniae using fluorescent dyes.* J Vis Exp, 2014(84): p. e51008.
57. Wenyun Lu, M.F.C., Eugene Melamud, Daniel Amador-Noguez, Amy A. Caudy, and Joshua D. Rabinowitz. , *Metabolomic Analysis via Reversed-Phase Ion-Pairing Liquid Chromatography Coupled to a Stand Alone Orbitrap Mass Spectrometer.* Anal. Chem., 2010. **82**: p. 3212–3221.
58. Melamud, E., L. Vastag, and J.D. Rabinowitz, *Metabolomic analysis and visualization engine for LC-MS data.* Anal Chem, 2010. **82**(23): p. 9818-26.
59. Clasquin, M.F., E. Melamud, and J.D. Rabinowitz, *LC-MS data processing with MAVEN: a metabolomic analysis and visualization engine.* Curr Protoc Bioinformatics, 2012. **Chapter 14**: p. Unit14 11.
60. Chong, J.S., O. Li, C. Caraus, I. Li, S. Bourque, G. Wishart, D. S. Xia, J., *MetaboAnalyst 4.0: towards more transparent and integrative metabolomics analysis.* Nucleic Acids Res, 2018. **46**(W1): p. W486-W494.
61. Joomi LEE, J.P., Mi-sun LIM, Sook Jin SEONG, Jeong Ju SEO, Sung Min PARK, Hae Won LEE, and Young-Ran YOON. , *Quantile Normalization Approach for Liquid Chromatography–Mass Spectrometry-based Metabolomic Data from Healthy Human Volunteers.* Analytical Sciences, 2012. **28**.

Figures

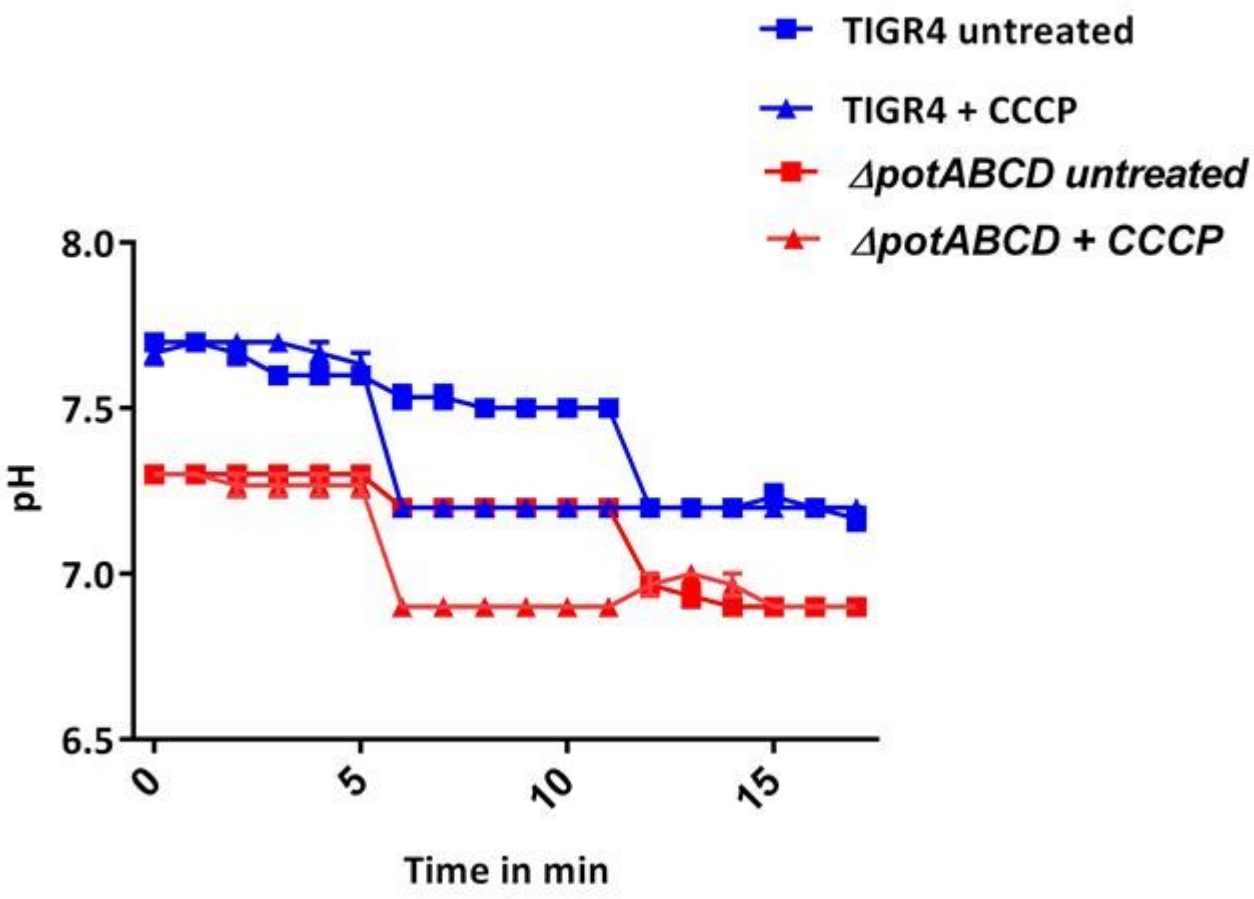

Figure 1

Intracellular pH of S. pneumoniae TIGR4 and ΔpotABCD. Three replicates of TIGR4 and ΔpotABCD were loaded with 5 mM of pH sensitive fluorescence dye BCECF-AM, washed with PBS, re-energized with 10% glucose, and baseline fluorescence readings were established in the first 5 mins. Controls were supplemented with 10 μM CCCP as a protonophore (triangles), and fluorescence of CCCP-treated controls and untreated samples (squares) was measured for an additional 5 mins. The pHi of untreated TIGR4 (blue squares) and ΔpotABCD (red squares) is 7.5 and 7.2, respectively. Nigericin (20 μM) was added to both treated and untreated samples to dissipate transmembrane gradients over that last 5 mins. Graphs represent the mean of three independent experiments

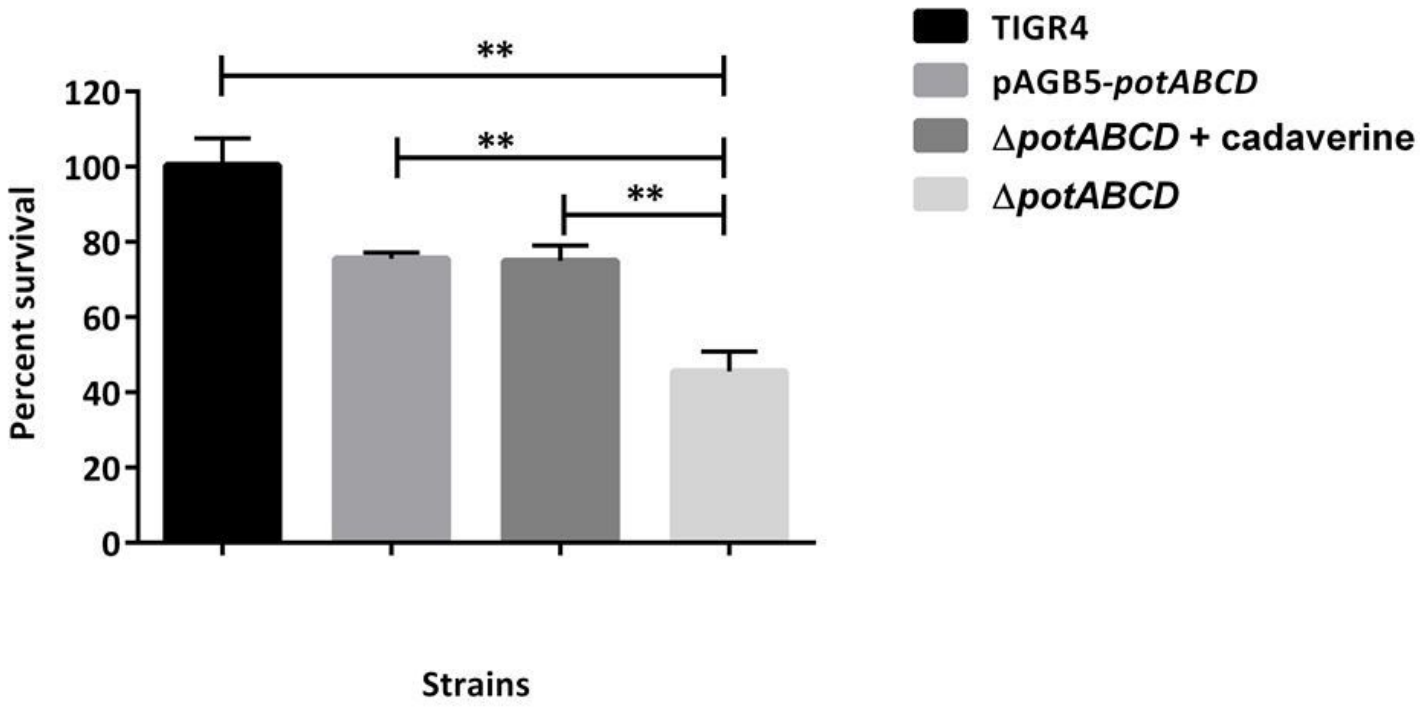

Figure 2

Hydrogen peroxide susceptibility of S. pneumoniae TIGR4, ΔpotABCD and pABG5-potABCD. The graph shows bacterial sensitivity to 2.5 mM H2O2 at 15 min post exposure. Also included is ΔpotABCD supplemented with cadaverine (¼MIC). The results represent an average of three independent experiments. Percentage survival relative to the untreated control is shown as a bar with the standard error of the mean, with ** representing $p \leq 0.01$, determined by a Student's T-test.

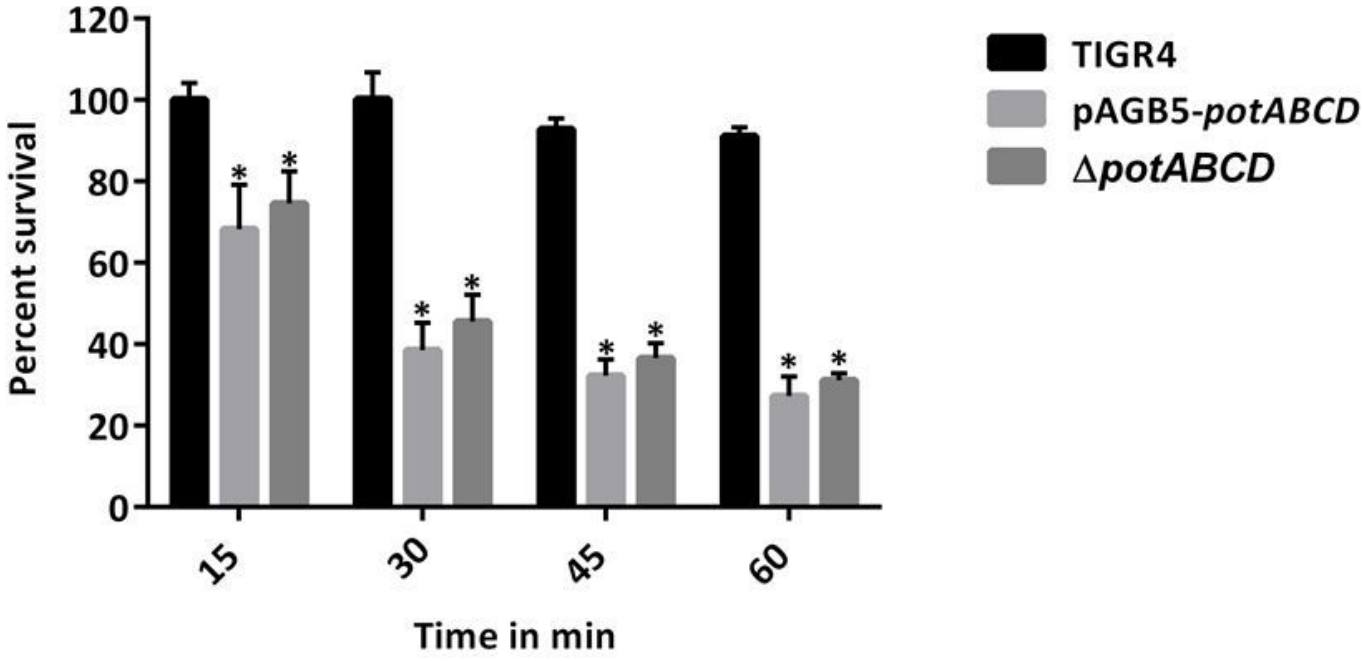

Figure 3

S-nitrosoglutathione susceptibility assay of S. pneumoniae TIGR4, ΔpotABCD and pABG5-potABCD. The graph shows bacterial sensitivity to 2.5 mM GSNO at 15-60 min post exposure. The results represent an average of three independent experiments. Percentage survival relative to the untreated control is shown as a bar with the standard error of the mean, with * representing $p \leq 0.01$ based on a Student's T-test.

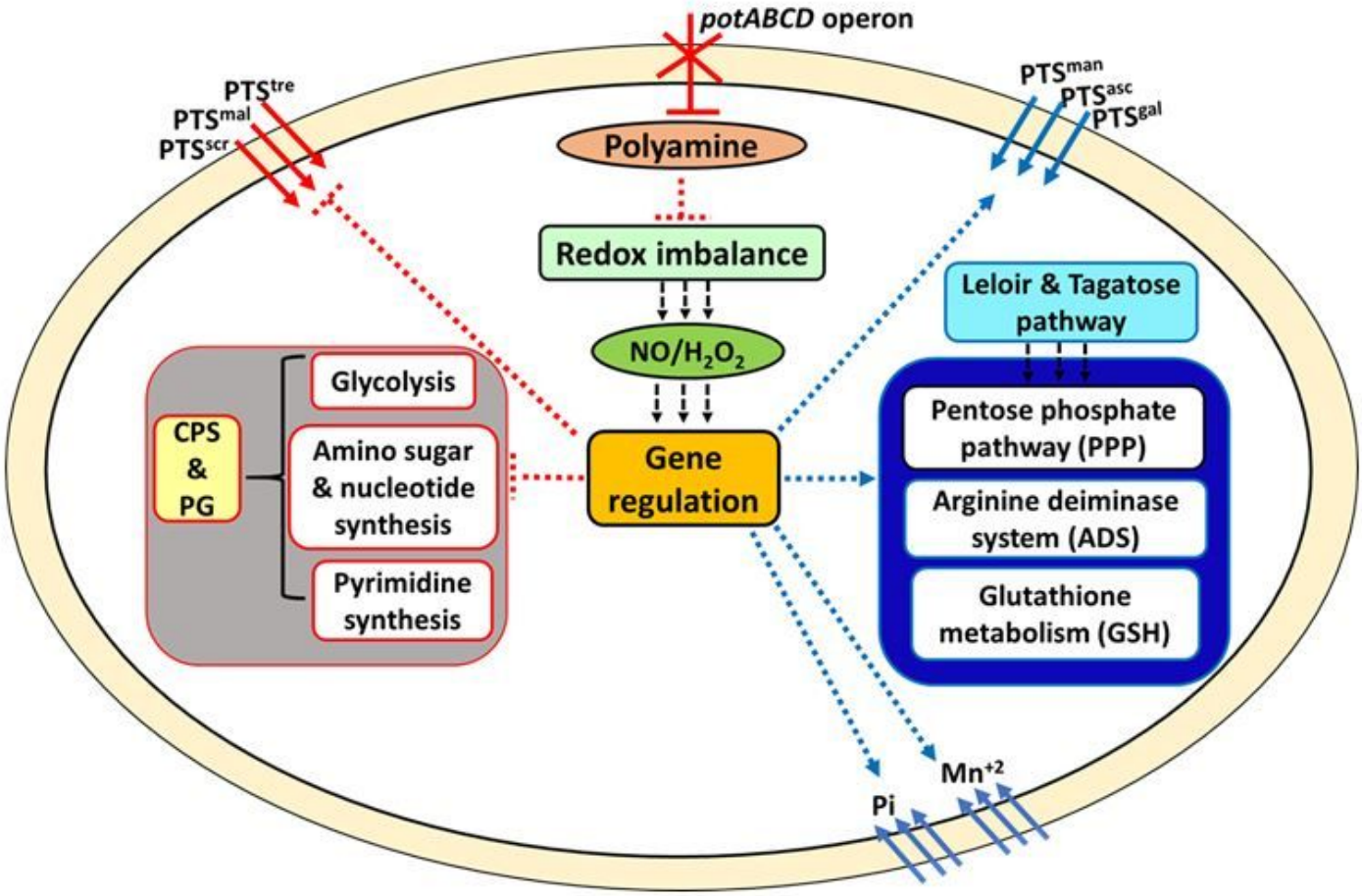

Figure 4

Intersection between polyamine metabolism, stress responses, carbohydrate metabolism and CPS/PG production in S. pneumoniae. Multi-step reactions are shown as dotted arrows, (blue represents upregulated while red represents downregulated reactions). Deletion of the polyamine transporter results in reduced intracellular polyamine levels (red oval), impairing the redox system (light green rectangle), rendering the pneumococci susceptible to NO and H2O2 stress (dark green oval). The stressful conditions alter gene regulation (orange rectangle) to limit processes (grey square; glycolysis, pyrimidine, and amino sugar nucleotide synthesis) that yield precursors for CPS and PG synthesis (yellow vertical rectangle). Reduced CPS, PG and protein synthesis could be to save energy for redox homeostasis (dark blue vertical rectangle; ADS, PPP, and GSH metabolism) and cation inflow. Influx of carbohydrates via phosphotransferase systems (PTS) that promote synthesis of glycolysis is inhibited in favor of inflow of carbohydrates that favor the Leloir pathway and tagatose pathways (light blue rectangle) probably to provide PPP intermediates.

Supplementary Files

This is a list of supplementary files associated with this preprint. Click to download.

- SupplementeryTable2.xls